GA–A27401

RELATING THE L-H POWER THRESHOLD SCALING TO EDGE TURBULENCE DYNAMICS

by

Z. YAN, G.R. MCKEE, J.A. BOEDO, D.L. RUDAKOV, P.H. DIAMOND, G. TYNAN, R.J. FONCK, R.J. GROEBNER, T.H. OSBORNE, AND P. GOHIL

OCTOBER 2012

GENERAL ATOMICS

DISCLAIMER

GA–A27401

RELATING THE L-H POWER THRESHOLD SCALING TO EDGE TURBULENCE DYNAMICS

by
Z. YAN[1], G.R. MCKEE[1], J.A. BOEDO[2], D.L. RUDAKOV[2], P.H. DIAMOND[2], G. TYNAN[2], R.J. FONCK[1], R.J. GROEBNER[3], T.H. OSBORNE[3], AND P. GOHIL[3]

This is a preprint of a paper to be presented at the 24th IAEA Fusion Energy Conference, October 8–12, 2012, in San Diego, California,.

[1]University of Wisconsin-Madison, Madison, Wisconsin, USA
[2]University of California San Diego, La Jolla, California USA
[3]General Atomics, P.O. Box 85608, San Diego, California USA

Work supported by
the U.S. Department of Energy
under DE-FG02-89ER53296, DE-FG02-07ER54917, and
DE-FG02-04ER54698

GENERAL ATOMICS PROJECT 30200
OCTOBER 2012

Relating the L-H Power Threshold Scaling to Edge Turbulence Dynamics

Z. Yan[1], G.R. McKee[1], J.A. Boedo[2], D.L. Rudakov[2], P.H. Diamond[2], G. Tynan[2], R.J. Fonck[1], R.J. Groebner[3], T.H. Osborne[3], and P. Gohil[3]

[1]*University of Wisconsin-Madison, Madison, Wisconsin 53706-1687, USA*
[2]*University of California San Diego, La Jolla, California 92093, USA*
[3]*General Atomics, P.O. Box 85608, San Diego, California 92186-5608, USA*

Abstract. Understanding the physics of the L-H transition power threshold scaling dependencies on toroidal field and density is critical to operating and optimizing the performance of ITER. Measurements of long-wavelength ($k_r\rho_I<1$) turbulent eddy dynamics, characteristics, flows, and flow shear in the near edge region of DIII-D plasmas have been obtained during an ion gyro-radius scan (varying toroidal field and current) and density scan in a favorable geometry (ion ∇B drifts towards the X-point), in order to determine the underlying mechanisms that influence the macroscopic L-H power threshold scaling relations. It is found that the integrated long wavelength density fluctuation amplitudes scale with ρ* approaching the L-H transition, suggesting a stronger drive of zonal flows that may trigger the transition at lower toroidal field. The turbulence poloidal flow spectrum evolves from Geodesic Acoustic Mode (GAM) dominant at lower power to Low-Frequency Zonal Flow (LFZF) dominant near the L-H transition, and the effective shearing rate correspondingly increases. An inferred Reynolds Stress, $\left\langle \tilde{v}_r(t)\tilde{v}_\theta(t)\right\rangle$, from BES velocimetry measurements is found to significantly increase near the L-H transition. Similar observations are made with the Langmuir probe measurements. At lower electron density, a clear increase of the LFZF is observed prior to the L-H transition, which is not evident at higher density. Taken together, these results are qualitatively/semi-quantitatively consistent with the electron density and toroidal field scaling of the L-H transition power threshold.

1. Introduction

Accessing H-mode and maintaining H-mode performance levels are critical to ITER operation. For years, work has focused on determining the requirements for access to H-mode in various machines. It has been found that the L-H transition power threshold increases with toroidal field and density, $P_{LH} = 0.049 B_t^{0.8} n_e^{0.72} S^{0.94}$ [1]. However, it has been found in many machines that there is a minimum in the density dependence of the power threshold. As the density is further lowered below a particular minimum value, the L-H transition power threshold increases. This density value corresponding to minimum power threshold may be a function of toroidal field. Besides the toroidal field and density dependence included in the well-known scaling relation, the L-H transition power threshold is also a strong function of toroidal rotation [2], ion species [3–5], divertor magnetic geometry [6], etc. The underlying physics behind these so-called "hidden parameters" has not been identified. Understanding such physics is clearly very important for achieving the high performance goals for ITER.

In order to investigate the physical mechanisms behind these dependencies, a set of L-H transition experiments has recently been performed on DIII-D that focuses on investigating the dependence of local edge parameters on toroidal field and density near the L-H threshold. These experiments were performed in favorable geometry (ion ∇B drifts towards the X-point) deuterium plasmas with scans of normalized ion gyroradius ($\rho^* = \rho_I/a$) and density. Turbulence dynamics and characteristics were measured at the plasma edge to investigate how the edge turbulence dynamics impact the L-H transition scaling. This paper presents the experimental conditions, turbulence characteristics and scaling behavior from these experiments and relates them to the L-H transition power threshold.

2. Experimental Set Up

The experiments for the ion gyroradius scan were performed with a downward biased double-null magnetic configuration. The direction of the applied toroidal magnetic field produced an ion grad-B drift towards the lower X-point. The toroidal field was varied from 1 T to 2 T with current ranging from 0.5 MA to 1 MA. The edge safety factor q_{95} was held nearly fixed at 5. The other non-dimensional parameters such as collisionality ν^*, T_e/T_i were kept nearly constant at the pedestal top in the L-mode phase just before the L-H transition by appropriately varying the injected beam power and the gas fueling. The L-H transitions were obtained by slowly increasing the NBI heating power.

A separate experiment was performed to vary density in a similar plasma shape at fixed toroidal field of 2 T and current of 1 MA. Line-averaged electron density in the L-mode phase before the L-H transition was varied from 1.7×10^{19} m^{-3} to 4.3×10^{19} m^{-3}. Figure 1(a,b) show some basic plasma parameters for these two experiments.

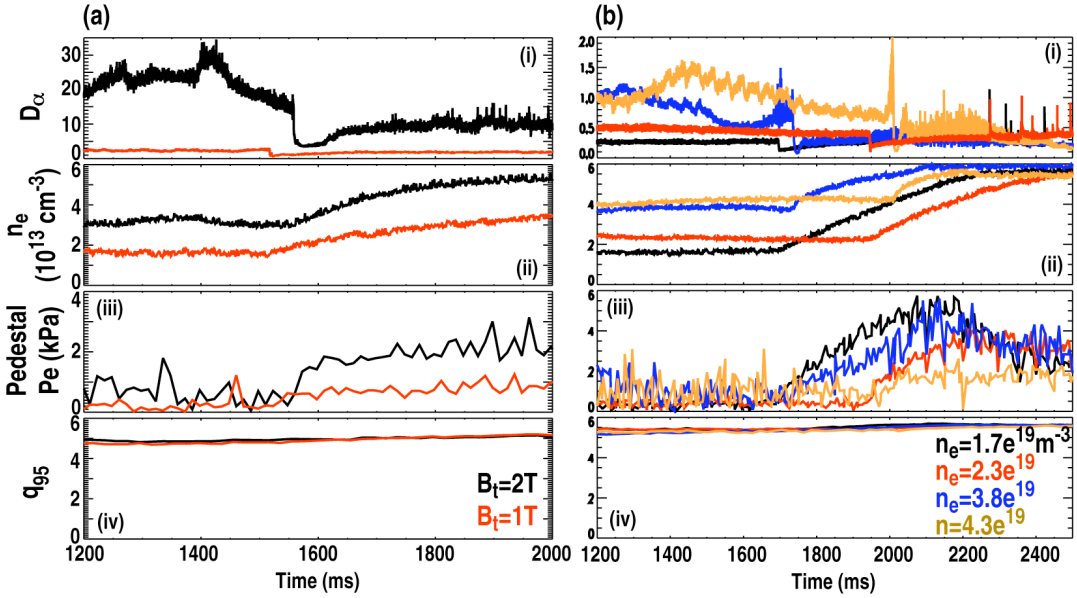

Fig. 1 (a) Ion gyroradius scan and (b) density scan basic parameters (i) D_α signal, (ii) line-averaged density, (iii) pedestal pressure and (iv) q_{95}.

For both experiments an 8×8 2D array of high sensitivity Beam Emission Spectroscopy (BES) viewchords was located in the plasma edge region (r/a~0.85–1.0+) providing long wavelength ($k_\perp \rho_I < 1$) density fluctuation measurements before, during and after the L-H transition. Figure 2 displays the plasma equilibrium plots for different parameter scans with the BES 2D array overlaid.

3. Toroidal Field Dependence of Power Threshold and Turbulence Dynamics

It is interesting to compare the turbulence dynamics at different times relative to the L-H transition for different plasma conditions. For this purpose long wavelength density fluctuation measurements from BES were analyzed for two toroidal fields (two ρ^* values) at two 10 ms time windows, one well before the L-H transition (~300 ms before) and the other near the L-H transition (10 ms before).

Figure 3 shows the profile of the relative density fluctuation amplitudes ($\tilde{n}/n$) integrated over 20–150 kHz (where broadband fluctuations exist) at the time near the transition for the two ρ^* values. It is found that the relative density fluctuation amplitudes scale with ρ^* approaching the L-H transition. This higher normalized turbulence amplitude at lower toroidal field (higher ρ^*) suggests a stronger drive for zonal flows, which are thought to play a dominant role in triggering the L-H transition [7].

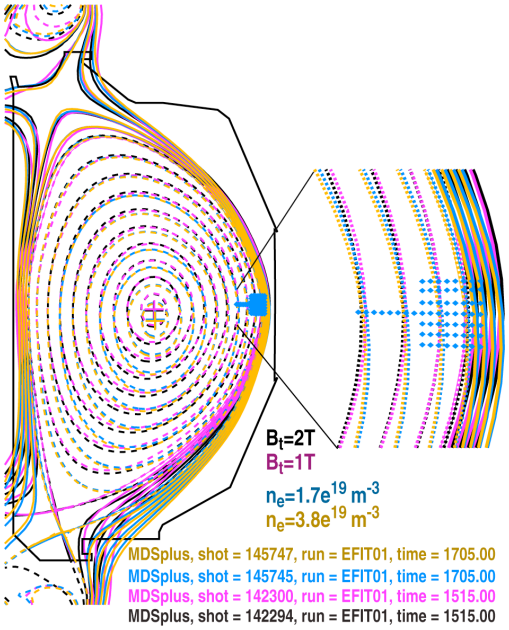

Fig. 2. Plasma equilibrium plots with BES array overlaid.

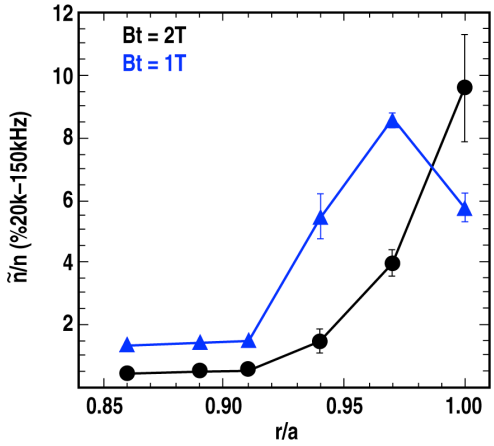

Fig. 3 Integrated density fluctuation amplitudes for B_t = 2 T (black) and B_t = 1 T (blue).

An imaging velocimetry technique [8] was applied to the 2D BES measurements to get the instantaneous radial and poloidal velocity fields of the turbulent eddy structures. The 2D BES density fluctuation measurements were first frequency filtered in a range of 50 kHz to 150 kHz for each spatial channel before the application of the velocimetry algorithm. Figure 4(a) shows an example of such a turbulent velocity field, indicated by the arrows overlaid on a one microsecond 2D BES density fluctuation image snapshot. To examine the turbulence and zonal flow dynamics, the poloidal velocity component from the velocimetry analysis is isolated and spectrally analyzed. The velocity spectrum of this turbulent velocity field is obtained via ensemble-averaging FFT power spectra over a 10 ms time window at different times relative to the L-H transition, as shown in Fig. 4(b,d) for both low and high ρ^* conditions. It is found that in both cases, an increase of the lower frequency component of the turbulence poloidal flow spectrum is observed as the discharge evolves from well before the L-H transition to near the transition. Furthermore, the velocity spectrum evolves from being Geodesic Acoustic Mode (GAM) dominant at lower input power to being Low-Frequency Zonal Flow (LFZF) dominant near the L-H transition. From the measured turbulence velocity field we can infer the Reynolds stress profiles $\langle \tilde{v}_r(t)\tilde{v}_\theta(t)\rangle$ at the different times and different ρ^*, which are shown in Fig. 4(c,e). It is found that the inferred Reynolds stress gradient increases in the pedestal region approaching the L-H transition for both cases.

The gradient of the Reynolds stress is predicted to drive zonal flows [7]. Similar observations were also made by the multi-tip reciprocating Langmuir probe measurements. The increase of the Reynolds stress gradient is consistent with the observation of the increase of LFZF-like flow component near the L-H transition in the context of theoretical predictions for L-H transition dynamics. The lower frequency and higher amplitude of the LFZF relative to the GAM suggests a stronger shear state near the transition [7], suggesting the observed increase in Reynolds stress and zonal flows may be playing a role in triggering the transition.

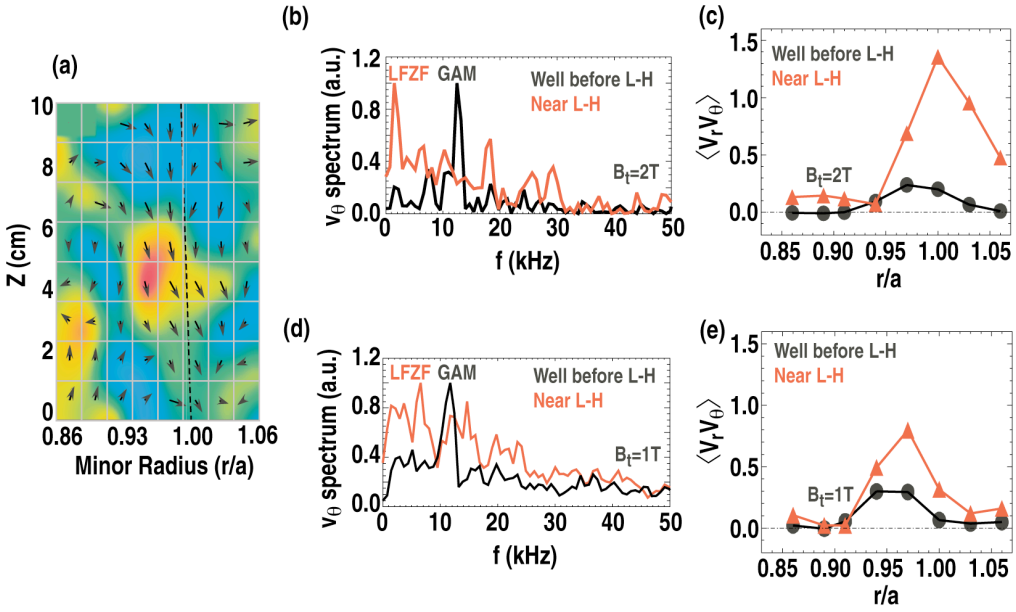

Fig. 4. (a) A snap shot of the density fluctuation imaging from 2D BES measurement overlaid by the turbulent velocities (black arrows) from velocimetry technique; turbulence poloidal flow spectrum at (b) B_t = 2 T and (d) B_t =1 T, and inferred Reynolds stress profile at (c) B_t =2 T and (e) Bt =1 T, with black for the time well before L-H transition and red for the time near transition.

The equilibrium turbulence poloidal flows were also obtained by taking a time average of the instantaneous poloidal velocity at the two 10 ms time windows. Figure 5 compares this time-averaged turbulence poloidal velocity for different times relative to the L-H transition for different ρ^* values. A significant increase of the equilibrium flow shear is clearly observed near the L-H transition relative to the earlier time. From this flow profile a shearing rate can be estimated as a gradient between the two adjacent radial positions. This shearing rate is compared with the decorrelation rate meas-ured from BES, which is shown in Fig. 6. It is found that the decorre-lation rate of the 50–150 kHz long wavlength density fluctuations does not change much with time. However, the shearing rate increases significantly

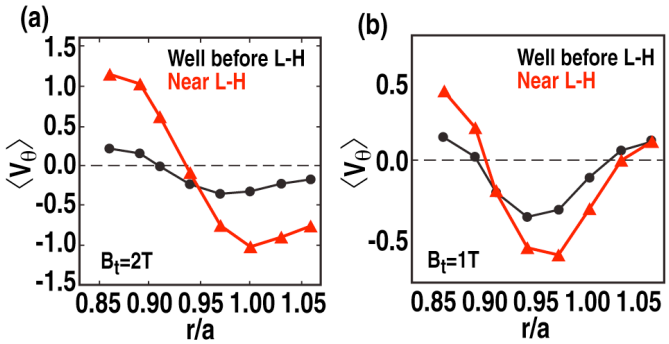

Fig. 5 (a) Equilibrium turbulence poloidal velocity profile at B_t =2 T for the time well before the L-H transition (black) and near the transition (red); (b) Equilibrium turbulence poloidal velocity profile at B_t = 1 T for the time well before the L-H transition (black) and near the transition (red).

approaching the L-H transition and exceeds the decorrelation rate. Therefore, the shearing rate is strong enough to suppress the turbulence and transport, consistent with triggering the L-H transition. It seems this happens for both low and high ρ^*. Therefore, this observation suggests that at high ρ^* (low toroidal fields), a lower input power manages to generate sufficient turbulence amplitude to drive a strong enough flow shear to trigger the L-H transition. GAM suggests a stronger shear state near the transition [7], suggesting the observed increase in Reynolds stress and zonal flows may be playing a role in triggering the transition.

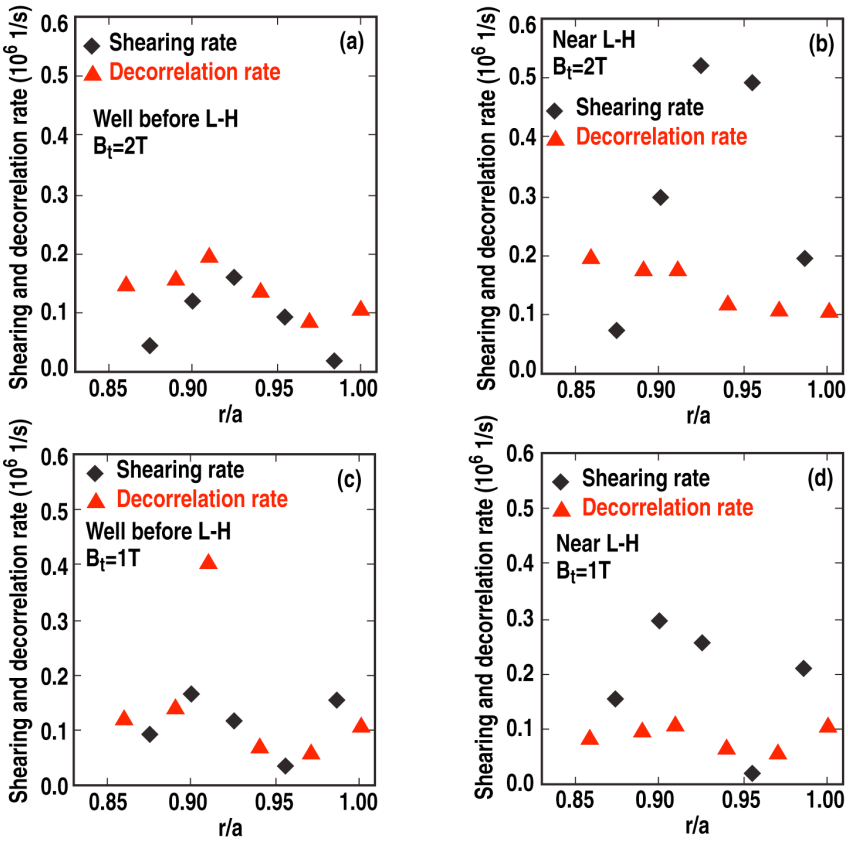

Fig. 6. Turbulence flow shearing rate (black diamond) and decorrelation rate (red triangle), both obtained from 2D BES turbulence measurements for (a) B_t = 2 T at time well before the transition; (b) B_t = 2 T at the time near the L-H transition; (c) B_t = 1 T at the time well before the transition and (d) B_t = 1 T at the time near the L-H transition.

The equilibrium turbulence poloidal flows were also obtained by taking a time average of the instantaneous poloidal velocity at the two 10 ms time windows. Figure 5 compares this time-averaged turbulence poloidal velocity for different times relative to the L-H transition for different ρ^* values. A significant increase of the equilibrium flow shear is clearly observed near the L-H transition relative to the earlier time. From this flow profile a shearing rate can be estimated as a gradient between the two adjacent radial positions. This shearing rate is compared with the decorrelation rate measured from BES, which is shown in Fig. 6. It is found that the decorrelation rate of the 20-150 kHz long wavelength density fluctuations does not change much with time. However, the shearing rate increases significantly approaching the L-H transition and exceeds the decorrelation rate. Therefore, the shearing rate is strong enough to suppress the turbulence and transport, consistent with triggering the L-H transition. It seems this happens for both low and high ρ^*. Therefore, this observation suggests that at high ρ^* (low toroidal fields), a lower input power manages to generate sufficient turbulence amplitude to drive a strong enough flow shear to trigger the L-H transition.

4. Density Dependence of Power Threshold and Turbulence Dynamics

A density scan was performed to examine the turbulence behavior approaching L-H transition as a function of density. In similarly shaped plasmas as used in the ρ^* scan experiment (B_t = 2 T and I_p = 1 MA), the line averaged density in the L-mode phase just before the L-H transition was varied over four values, 1.7×10^{19}m^{-3}, 2.3×10^{19}m^{-3}, 3.8×10^{19}m^{-3} and 4.3×10^{19} m^{-3}. Applying the same velocimetry technique described in the previous section to the 2D BES density fluctuation measurements, we again obtained the instantaneous radial and poloidal velocity fields. Figure 7 shows the spectra of the turbulence poloidal velocity field. It is found that for the low-density cases (1.7–2.3$\times10^{19}$ m^{-3}) there is a clear increase of the LFZF-like flow component as the plasma evolves towards the L-H transition. The spectra again evolve from being GAM dominant to being LFZF dominant near the transition, as seen in the ρ^* plasmas. However, there is no evident observation of increase of the LFZF-like flow component at the higher density cases (3.8–4.3$\times10^{19}$ m^{-3}). Moreover, no GAM was observed at these higher densities, which may be consistent with the higher collisional damping of the zonal flows at higher density.

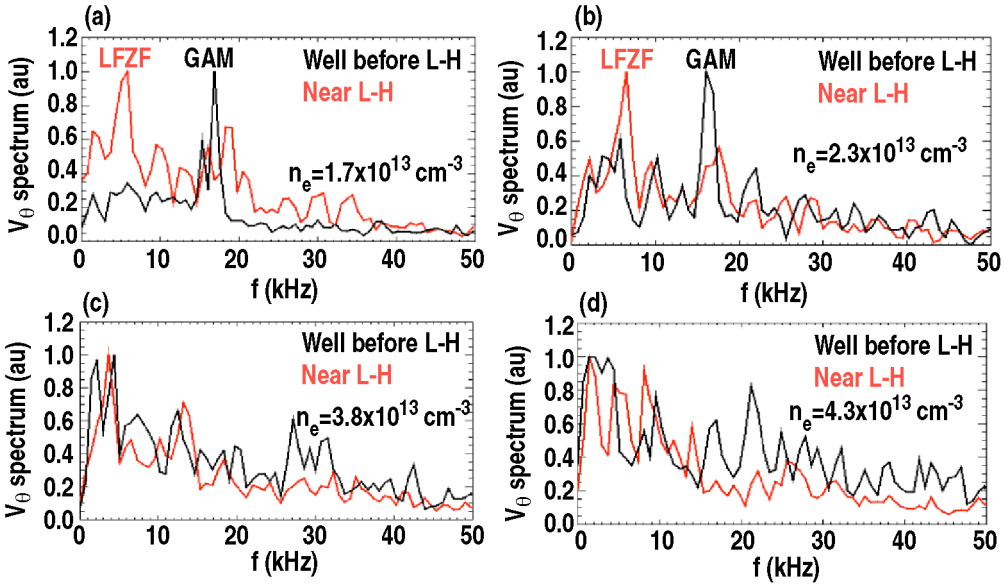

Fig. 7. Spectrum of the turbulence poloidal velocity field for (a) n_e = 1.7x10^{19} m^{-3}, (b) n_e = 2.3x10^{19} m^{-3}, (c) n_e = 3.8x10^{19} m^{-3}, and (d) n_e = 4.3x10^{19} m^{-3}. For each panel black is the time well before the L-H transition and red is for the time near the transition.

The equilibrium turbulence poloidal flow at the time near the L-H transition was obtained by evaluating the time delay cross correlations between the poloidally separated BES density fluctuation measurements. Figure 8 is a plot of the profile of such flow for the four different densities. It is clearly seen that at two lower densities there is a much higher shear around r/a~0.9 than that at two higher densities, with the local shearing rate exceeding the turbulence decorrelation rate. These observations suggest that the combination of the increased turbulence flow shear and zonal flow shear at lower density facilitate the L-H transition at lower density, consistent with the P_{LH} scaling relation.

5. Summary

These results of the edge turbulence dynamics scaling with toroidal field and density across the L-H transition are qualitatively and semi-quantitatively consistent with the density and toroidal field scaling of the L-H transition power threshold. A consistent picture of the behavior of the turbulence-zonal flow system is found as the L-H transition is approached. At lower toroidal field (higher ρ^*), larger normalized turbulence amplitude is generated, which is predicted to drive stronger zonal flows and corresponding flow shear which can facilitate the L-H transition at the lower input power. Similarly, the stronger flow shear observed at lower density favors the L-H transition at correspondingly lower input power. It appears that increased turbulence at high power flux drives a stronger Reynolds stress; the Reynolds stress gradient then drives increased zonal flows, which can then trigger the L-H transition through shear flow decorrelation of turbulence. Future studies will include investigating the turbulence dynamics corresponding to the previously observed increase of the L-H transition power threshold with density falling below the minimum power threshold value. Other factors like the X-point height dependence and edge neutral recycling, etc. will also be investigated.

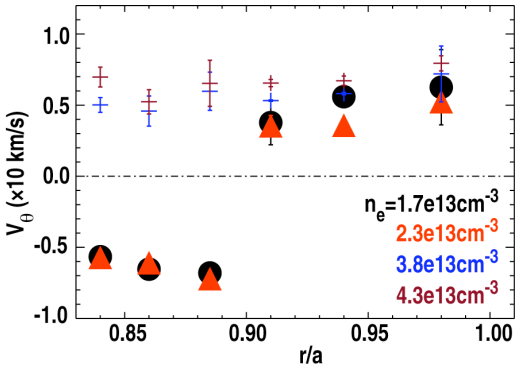

Fig. 8. Turbulence poloidal flow profiles for different densities near L-H transition.

This work was supported by the US Department of Energy under DE-FG02-89ER53296, DE-FG02-07ER54917, DE-FG02-06ER54871, and DE-FC02-04ER54698.

References

[1] DOYLE, E.J., et al., Nucl. Fusion **47** (2007) S18
[2] MCKEE, G.R., et al., Nucl. Fusion **49** (2009) 115016
[3] GOHIL, P., et al., Nucl. Fusion **49** (2009) 115004
[4] GOHIL, P., et al., Nucl. Fusion **50** (2010) 064001
[5] RYTER, F., et al., Nucl. Fusion **49** (2009) 062003
[6] CARLSTROM, T.N., et al., Plasma Phys. Control Fusion **40** (1998) 669
[7] DIAMOND, P.H., et al., Plasma Phys. Control Fusion **47** (2005) R35
[8] McKEE, G.R., et al., Rev. Sci. Instrum. **75** (2004) 3490